Pakistan Veterinary Journal

ISSN: 0253-8318 (PRINT), 2074-7764 (ONLINE)
DOI: 10.29261/pakvetj/2024.219

RESEARCH ARTICLE

Novel Effect of Red Grape Seed Extract in Repairing Intercellular Junction in Reticuloendothelial Organs

Snur Mohemmed Amin Hassan*

Department of Anatomy and Pathology, College of Veterinary Medicine, University of Sulaimani, 4601, KRG/Iraq
*Corresponding author: snur.amin@univsul.edu.iq, hassan_snur@yahoo.com

ARTICLE HISTORY (24-199)

Received: April 05, 2024
Revised: July 19, 2024
Accepted: July 24, 2024
Published online: August 07, 2024

Key words:
Claudin-1
Claudin-5
E-cadherin
Interstitial nephritis
Lymphocytic hyperplasia
Tight junction

ABSTRACT

Polyphenols and phenolic acids make up the majority of the complex mixture of compounds, such as grape seed extract (GSE). In this study, the protective effects and working mechanisms of Red Grape Seed extract (GSE) against ethanol (EtOH)-induced tight junction (TJ) and adherent junction protein dysfunction were investigated in the rats' liver, kidney, and spleen. Twenty-four adult Albino Sprague Dawley rats were used and divided into 4 groups: Group 1 (Control Negative), and Group 2 (Control Positive), the rats received a twice-weekly dosage of 40% ethanol; In Group 3, rats were given Red GSE only; Group 4 (treatment group), rats were given EtOH + Red GSE, which was administered three times weekly orally through gavage tube for six weeks. The liver, kidney, and spleen tissue were processed for the H&E staining and Claudin-1, Claudin-5, and E-cadherin biomarkers by IHC analysis. Treatment with Red GSE reduced the histopathologic abnormality scores in the liver (7 vs. 13), kidney (2 vs. 8), and spleen (3 vs. 6) when compared to the EtOH group, which alleviated the harmful effects of EtOH. Additionally, Red GSE increases the expression of Claudin-1, Claudin-5, and E-cadherin by a membrane pattern in the parenchyma of the liver, kidneys, and spleen, mostly by moderate-strong immunostaining in contrast to EtOH, which displayed weak staining in membranous and cytoplasmic regions. Red GSE preserves the tight junction in the damaged cells and is a promising natural agent against ethanol-induced barrier dysfunction.

To Cite This Article: Hassan SMA, 2024. Novel effect of red grape seed extract in repairing intercellular junction in reticuloendothelial organs. Pak Vet J, 44(3): 657-666. http://dx.doi.org/10.29261/pakvetj/2024.219

INTRODUCTION

Global alcohol consumption and abuse are currently quite prevalent. Nine hundred million women and 1.5 billion men were among the estimated 2.4 billion individuals who drank alcohol globally in 2016 (Ramkissoon and Shah, 2022). Alcoholic liver disease (ALD), the leading cause of liver-related morbidity and mortality worldwide, is estimated to have developed in around 20% of chronic alcohol consumers (Nagy *et al.*, 2016). The etiopathogenesis of ALD is complex. ALD is caused by a combination of genetic, environmental, and metabolic processes that occur after heavy alcohol consumption. Hepatocyte damage was generated by increasing ethanol through the generation of reactive oxygen species (ROS), endoplasmic reticulum (ER) stress, and mitochondrial dysfunction (Mukherji *et al.*, 2019). Due to the increased permeability caused by ethanol, the damaged hepatocytes release molecules known as danger-associated molecular patterns (DAMPs) and pathogen-associated molecular patterns (PAMPs), which draw neutrophils into the liver and cause liver inflammation. These molecules are thought to be essential in the development of alcoholic liver disease (ALD) (Shim and Jeong, 2020).

Chronic alcoholism is also linked to chronic kidney disease (Li *et al.*, 2022). It is the development of acute kidney injury (AKI) that is associated with the mortality of alcoholic hepatitis (Altamirano *et al.*, 2012). When rats are given ethanol in quantities that are comparable to chronic ethanol use, the kidneys are physically damaged (Hassan *et al.*, 2015). The term acute kidney injury (AKI) describes the sudden loss of renal filtration in addition to the blood's retention of nitrogenous waste products, such as blood urea nitrogen (BUN), which is linked to the development of AKI and the mortality rate from alcoholic hepatitis (Tamargo *et al.*, 2024).

Tight junctions (TJs), adherens junctions (AJs), desmosomes, and gap junctions are the four types of intercellular junctions (Chiasson-MacKenzie and

McClatchey, 2018). TJ proteins have been demonstrated to modulate inflammatory responses, cell migration, proliferation, and death through the coordination of inside-out and outside-in signaling (Singh *et al.*, 2017). TJ protein malfunction or downregulated expression has repeatedly been associated with chronic liver diseases (Zeisel *et al.*, 2019). One common symptom in mouse models of chronic liver injury is the loss of the Blood-Biliary Barrier (BBB), which is kept in place by junctional adhesion complexes made up of TJs (Pradhan-Sundd *et al.*, 2018). Claudins regulate renal paracellular permeability through their segmental expression in kidney tubular cells. Tight junctions are frequently seen under standard settings, but they grow and become prominent in nephrosis (Koda *et al.*, 2011).

The main functions of AJs and desmosomes are cell-cell adhesion and resistance to mechanical forces. They also aid in developing cell polarity, differentiation, and survival, which is ultimately necessary for preserving tissue integrity (Müller *et al.*, 2021). E-cadherin is expressed by cholangiocytes and periportal hepatocytes in mice, but not by perivenous hepatocytes (Hintermann and Christen, 2019). In addition to E-cadherin interiorization, prolonged ischemia injury also causes site-specific protein degradation and the disintegration of the cadherin-catenin connection. In renal epithelial ischemia, E-cadherin degradation, and cadherin-catenin interaction disruption are likely to be significant injuries (Menezes *et al.*, 2017).

The second most widely produced organic product in the world is the grape (*Vitis vinifera L.*), typically consumed raw, dried or matured into wine. Due to its high polyphenolic content, nutritional value, and natural acid content, grapefruit is used in natural remedies (Benmeziane *et al.*, 2014). Grapes, their seeds, leaves, and pomace are rich sources of monomeric phenolic chemicals called epicatechins, procyanidins, and catechins (Surai, 2014). Polyphenols have been viewed as neuroprotective, calming, hostile to cholinesterase, anti-amnesic, hypolipidemic, and anti-aging agents due to their various (pleiotropic) natural activities and possible health-promoting benefits (Zhang *et al.*, 2015).

Consequently, whether Red GSE has a protective effect against Ethanol-induced inflammatory reaction and damage by regulating intercellular junction is of interest. The current study was designed to close this knowledge gap. This study attempts to address the regulation of the junction complex components, including Claudin-1, Claudin-5, and E-cadherin, for the first time. This may help better understand the biology of ethanol-induced disease and may facilitate the therapeutic approach.

MATERIALS AND METHODS

Grape seed extraction and GC-MS analysis: *Vitis vinifera* red grape was used in this study and collected from Sharbazher village near Sulaimani city of the Kurdistan Region. The grape seed was removed after peeling the skin, then dried in the open air away from sunlight, and then the seed was extracted according to a study by Hassan *et al.* (2021).

Through the use of gas chromatography-mass spectrometry (GC-MS), the compounds present in purified samples of red grape seed (*Vitis vinifera*) from Sulaimania (Sharbazhear-Kurdistan region) were identified. As mentioned earlier by Hassan *et al.* (2021), >90% of net dry weight was comprised of total polyphenols (Hassan *et al.*, 2021).

Experimental animals and design: Twenty-four adult Albino *Sprague Dawley* rats, both male and female, weighing 250-300g, were utilized; they were between 6 and 8 weeks old. This study was carried out at the animal house of the Veterinary Teaching Hospital, College of Veterinary Medicine at the University of Sulaimani. Six animals in each group were retained in each plastic cage throughout the experiment housed in typical lab conditions, including a 12:12 light/dark photoperiod at a temperature of 23-25°C. Access to food and water was unrestricted for the animals. The study received approval from the local ethical committee for animal experimentation at the College of Veterinary Medicine at the University of Sulaimani (permit 030513, 9 March 2023).

Four groups were randomly assigned the animals, each with six rats. In group 1 (Control negative), rats of this group were not given any treatment. In group 2 (Control positive), the animals were provided liquid with ethanol 40% (v/v), twice a dose/week (Hassan *et al.*, 2015). Ethanol is from Vitane Pharmaceutical Inc., USA. In Group 3 (Control Treatment), rats were treated with Red GSE (600 mg/kg/day), and in Group 4 (Treatment group), rats were treated with EtOH+ Red GSE (600 mg/kg/day), the Red GSE was given in a three-dose/week orally. This study was performed for about six consecutive weeks.

Tissue sample collection for histologic examination: After giving the rats anesthesia with intraperitoneal (IP) ketamine (50mg/kg) and xylazine (5mg/kg), the rats were anesthetized. From each rat for each group, the liver, kidney, and spleen tissues were sampled for the study. The specimens were fixed for at least 48 hours in 10% neutral buffered formalin (NBF), then dehydrated in a graded series of ethanol, samples were embedded in paraffin, and sections were deparaffinized in Xylene and then consecutively hydrated in 100%, 95%, 70%, and 60% ethanol followed by two washes in Phosphate buffered saline (PBS) in the Histopathology Lab of Anwar Shexa Medical City/Sulaimani Governorate, four thin sections (4µm) from each tissue were mounted on normal and positively charged glass slides for hematoxylin and eosin (H&E) staining, also for an IHC marker including; E-cadherin, Claudin-1, and Claudin-5 markers.

Histopathologic assessment: A histopathologist evaluated the slides in a descriptive-analytical study using an Olympus light microscope (Japan) at 100X and 400X magnification to determine the severity of the liver, kidney, and spleen parenchyma. Using an (Amscope™, Japan), histological sections were inspected and captured with a camera linked to a computer. By calculating the percentage of the damaged area as shown in Tables 1-3, the extent of damage to the liver, kidney, and spleen was evaluated semi-quantitatively following the procedure by Hassan *et al.* (2022).

Table 1: Score assessment of the liver's histological features (Hassan *et al*., 2022).

Locations	Histopathologic abnormalities	Scores	Interpretation
Hepatic vasculature	*Congestion*	0	Absence of Change
	and	1	Change in less than 25% of vasculature
	Hemorrhage	2	Change in 26-50% of vasculature
		3	Change in 51-100% of vasculature
Hepatocytes	*Cellular Swelling*	0	Absence of Change
	and	1	Change in less than 25% of parenchyma
	Hydropic degeneration	2	Change in 26-50% of parenchyma
		3	Change in 51-100% of parenchyma
Kupffer cells	*Proliferation*	0	Absence of Change
	Mild	1	Change in less than 25% of cell
	Moderate	2	Change in 26-50% of cell
	Severe	3	Change in 51-100% of cell
Parenchyma	*Inflammation*	0	Absence of Change
Inflammation	*Mild*	1	Change in less than 25% of parenchyma
	Moderate	2	Change in 26-50% of parenchyma
	Severe	3	Change in 51-100% of parenchyma

Table 2: Evaluation score of histopathological characteristics in the kidneys (Hassan *et al*., 2022).

Locations	Histopathologic abnormalities	Scores	Interpretation
	Inflammation	0	Absence of Change
	Mild	1	Change in less than 25% of the glomerulus
	Moderate	2	Change in 26-50% of glomerulus
	Severe	3	Change in 51-100% of glomerulus
Glomerulus	Degeneration/Necrosis; Mild	0	Absence of Change
	Moderate	1	Change in less than 25% of the glomerulus
	Severe	2	Change in 26-50% of glomerulus
		3	Change in 51-100% of glomerulus
Tubular		0	Absence of Change
Compartment	Hydropic degeneration	1	Mild changes
	Nuclear changes	2	Moderate Changes
	Desquamation	3	Severe changes
Interstitial	*Congestion*	0	Absence of Change
Compartment	*and*	1	Change in less than 25% of interstitial tissue
	Hemorrhage	2	Change in 26-50% of interstitial tissue
		3	Change in 51-100% of interstitial tissue

Table 3: Score system for the spleen's histological features assessment (Hassan and Hassan, 2018).

Locations	Histopathologic abnormalities	Scores	Interpretation
	Lymphocytic hyperplasia	0	Absence of hyperplasia
White pulp	Mild	1	Hyperplastic changes about 25% of pulp
	Moderate	2	Hyperplastic changes about 26-50% of pulp
	Severe	3	Hyperplastic changes about 51-100% of pulp
	Congestion	0	Absence of Change
	and	1	Change in less than 25% of Red pulp
Red pulp	*Hemorrhage*	2	Change in 26-50% of Red pulp
		3	Change in 51-100% of Red pulp
	Inflammation	0	Absence of Change
	Mild	1	Change in less than 25% of Red pulp Change in 26-50% of Red
	Moderate	2	pulp
	Severe	3	Change in 51-100% of Red pulp

Immunohistochemical analyses: Tissue sections were treated with 10mM citrate buffer (pH 6.0) at 95-100°C for 20 min for antigen retrieval in a microwave oven, then treated with peroxidase block for 15 min, non-specific bindings were blocked with 5% bovine serum and 0.1% Triton X-100 in PBS before incubation with polyclonal primary anti-Claudin-1 and Claudin-5 antibodies (1:600, DAKO, Denmark) and polyclonal anti- E-Cadherin antibody (1:400, DAKO, Denmark) for 1 hr. After 3 washes in PBS, the sections were incubated with biotinylated secondary antibody for 30 min followed by (Horse radish Peroxidase-streptavidin, DAKO, Denmark) HRP for 60 min. After washing in PBS, the sections were treated with diaminobenzidine substrate-chromogen solution for 2-5 min at room temperature to see the reaction products (DAKO, Denmark). Finally, sections were Hematoxylin counterstained, dehydrated as per the usual method, and mounted with the mounting medium before being coated with coverslips.

The membrane and cytoplasm were stained with brownish granules of Claudin-1, Claudin-5, and E-Cadherin, respectively, while the nuclei were not stained, retaining their bluish color. Slices were examined under a microscope using computer-aided image analysis software (Motic, Japan) (Am Scope™ Version 2.5 software, Japan). A microscope examined each part of the liver, kidney, and spleen at 100 and 400X magnification.

To quantify the percentage of positively stained epithelial cells in IHC staining of Claudin-1, Claudin-5, and E-Cadherin, the previous scoring system described by Menezes *et al.* (2017) with modifications was used; In evaluating IHC sections, the relative percentage of immunopositive cells concerning the total number of target cells were assessed. Each value is recorded as a numerical score, for 5% positive staining recorded as (0), (1) for 5-25% positive staining, (2) for 25-50% positive staining, (3) for 50-75% positive staining, and (4) for >75% positive staining, intensity of the staining is also evaluated. The

intensity is commonly scored from 0 to 5; 0 for negative stain, weak (+1), weak-moderate (+2), moderate (+3), moderate-strong (+4), and strong (+5), Claudin-1, Claudin-5, and E-Cadherin staining intensity. The overall staining score ranged from 0 to 20 and was calculated by multiplying the extent of positive reactivity and the level of staining intensity referred to (Mustafa *et al.*, 2022) with modification.

RESULTS

Attenuation of Red GSE on the liver damage: Histopathologic evaluation of liver sections of rats in different groups showed that the control negative revealed (score 0) with normal histologic features and organization of central vein, the row of hepatocytes that arranged as bricks with sinusoidal capillaries and normal range of cellularity (Fig. 3a). The liver section revealed severe damage in all parenchyma with the highest lesions score vs. control negative group (13 vs. 0) as shown in (Fig. 1), which characterized by marked hepatic necrosis that revealed swollen hepatocyte with eosinophilic cytoplasm and nuclear karyorrhexis features, infiltration of mononuclear inflammatory cells throughout liver parenchyma particularly giant cells filtration (single huge cell with multiple nuclei), marked proliferation of Kupffer cells, and distention of sinusoidal capillary filled with inflammatory cells and RBC vs. control negative group (Fig. 3d,e). The liver section in the EtOH+ Red GSE treated group alleviated the liver damage by administration of Red GSE and also reduced score lesion vs. control positive group (5 vs. 12), and microscopically revealed mild congestion of central vein, marked hydropic degeneration of hepatocytes with narrowing of sinusoidal capillary, and reduced proliferation of Kupffer cells (Fig. 4a & b). While, the liver section in the control treatment group showed mild swelling of hepatocytes only with intact organization vs. the control negative group (Fig. 4f & g), which recorded a mild score in comparison to the control negative group (score 1 vs. 0) as seen in Fig. 1.

Red GSE's protective effects against kidney injury induced by ethanol: According to the histopathologic assessment of rat kidney sections in several groups. The control negative was recorded (score 0, Fig. 2) with typical histologic characteristics; well-organized glomeruli structures, intact collecting tubules, and normal renal vasculature with interstitial tissues (Fig. 3b). While kidney sections in the control positive group got a higher score of lesions than the control negative group (8 vs. 0) and showed severe pathologic alteration due to the effect of EtOH that displayed severe renal vascular congestion with interstitial hemorrhage, marked chronic interstitial nephritis with giant cells infiltration, focal-atrophy of glomeruli and dilation of urinary space vs. control negative group as shown in (Fig. 3f & g). The treatment group improved the kidney injury by administration of Red GSE vs. the control positive group. It lowered the score lesion (2 vs. 8) and microscopically showed moderate degeneration of collecting tubules with mild interstitial hemorrhage only (Fig. 4c & d). The kidney parenchyma of the control treatment group resembled normal histological structures when compared to the control negative group,

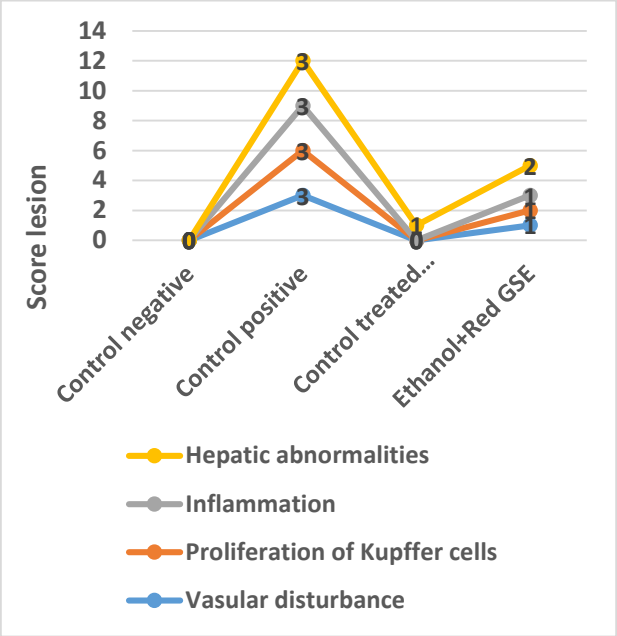

Fig. 1: The column chart shows scores of lesions in liver parenchyma among studied groups.

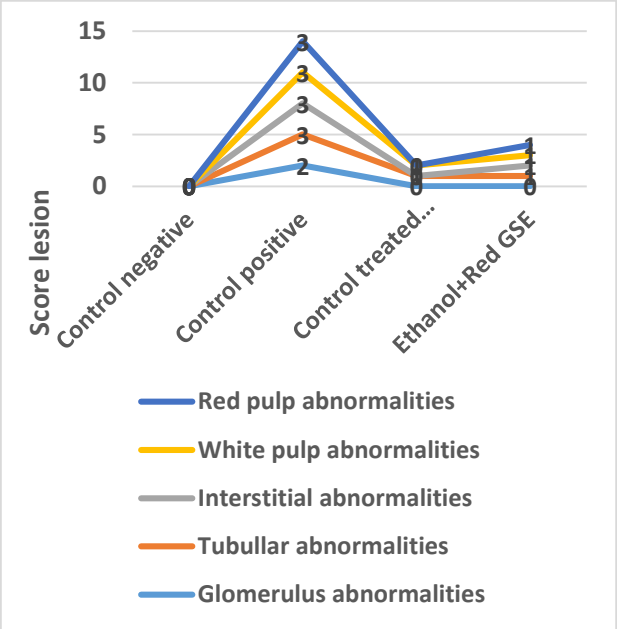

Fig. 2: Column chart revealed scores abnormalities in kidney and splenic parenchyma among studied groups.

and Red GSE did not have any harmful impacts on these structures (Fig. 4g). Similarly, the treated group's scoring lesion was also within the normal range (score 1 vs. 0).

The benefits of Red GSE in preventing EtOH-induced spleen damage: The control negative group's spleen section displayed normal cellularity in addition to normal white pulp and red pulp organization and intact histological characteristics (Fig. 3c). The spleen's histological abnormalities in the group that received EtOH treatment showed marked lymphocytic hyperplasia of white pulp with severe congestion, and hemorrhage of red pulp associated with mononuclear inflammatory infiltration with typical giant cells (Fig. 3h & i). In the treatment group (Fig. 4e), a marked decrease in splenic

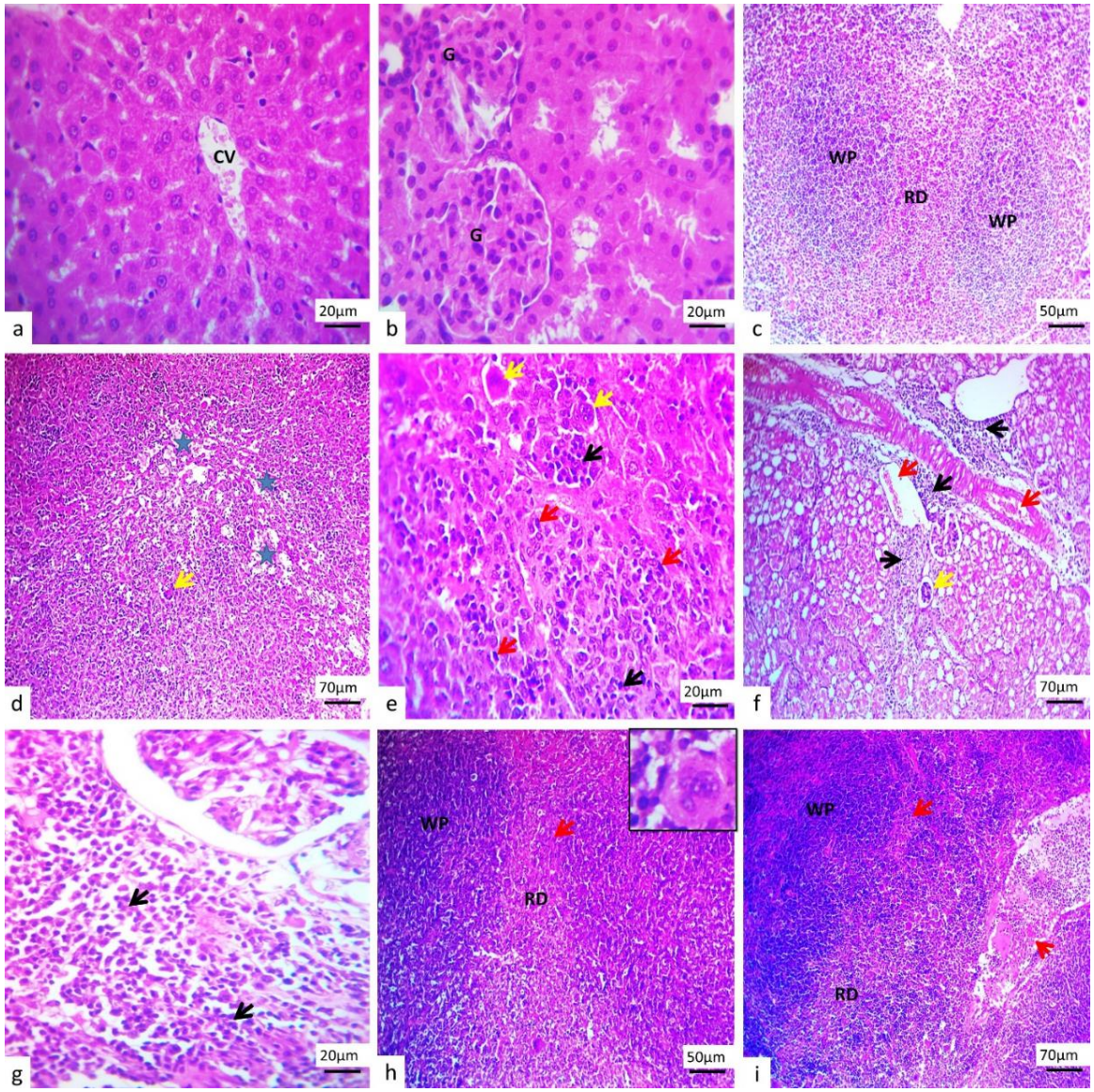

Fig. 3: Light microscopy of histological liver, kidney, and spleen sections of rat in control negative and positive groups showed; a: Normal histological features of liver parenchyma central vein (CV), rows of hepatocytes that separated by sinusoidal capillary in control negative group, b: Well-organized, intact glomeruli (G) and collecting tubules in control negative group, c: Normal architecture of splenic tissue of white and red pulp with cellularity and vasculatures in control negative group, d and e: Marked hepatic necrosis with karyorrhexis features associated with severe chronic inflammatory reaction (black arrows), and giant cells (yellow arrow), severe dilation of sinusoidal capillary (stars), and proliferation of Kupffer cells as indicated by red arrows in control positive group, f and g: Severe dilated renal vasculature (red arrows) with interstitial hemorrhage, marked interstitial nephritis (black arrows), focal-atrophy of glomeruli (yellow arrow), and dilation of urinary space in control positive group, h and i: Marked lymphocytic hyperplasia of white pulp with severe congestion (red arrows), and hemorrhage of red pulp associated with chronic inflammatory reaction with giant cells as indicated by inset in control positive group, (H&E stain).

alteration was seen vs. the control positive group, which only showed moderate lymphocytic hyperplasia of white pulp with mild congestion in the red pulp (Fig. 4e). Additionally, the rats that were treated with Red GSE only revealed normal cellularity and vasculature of splenic parenchyma vs. the control positive group (Fig. 4i). Concerning the total scoring of splenic injury, the Red GSE dropped the splenic lesions that induced by EtOH vs. control positive group, (2 vs. 6), respectively, while in comparison to the control negative group the scores in both groups were increased as shown in Fig. 2.

Immunohistochemical interpretation: The results of immunohistochemical staining cellular junction biomarkers including Claudin-1, Claudin-5, and E-cadherin are given in Fig. 5 and 6.

There was no immunopositive reaction for Claudin-1 (score 0) in all organs in the control negative group as shown in (Fig. 5a), particularly in the renal parenchyma. Whereas there was a focal weak (score 1) immunostaining of claudin-5 at the membranous endothelium of sinusoidal capillary and hepatocyte (Fig. 5b) vs. kidney and spleen that revealed no positive cell staining. Furthermore, the E-cadherin showed no staining (score 0) (Fig. 5c).

In the control positive group, there was weak-moderate brownish stain immunoreactivity (score 6) to antigens of claudin-1 diffusely distributed in the hepatocyte membrane and endothelium of sinusoidal capillary (Fig. 5d) vs. to the moderate staining of claudin-5 (score 9) that diffusely distributed in the cytoplasm of hepatocytes and the endothelium of the sinusoid (Fig. 5e). The scores of E-cadherin expressions in the liver section showed moderate

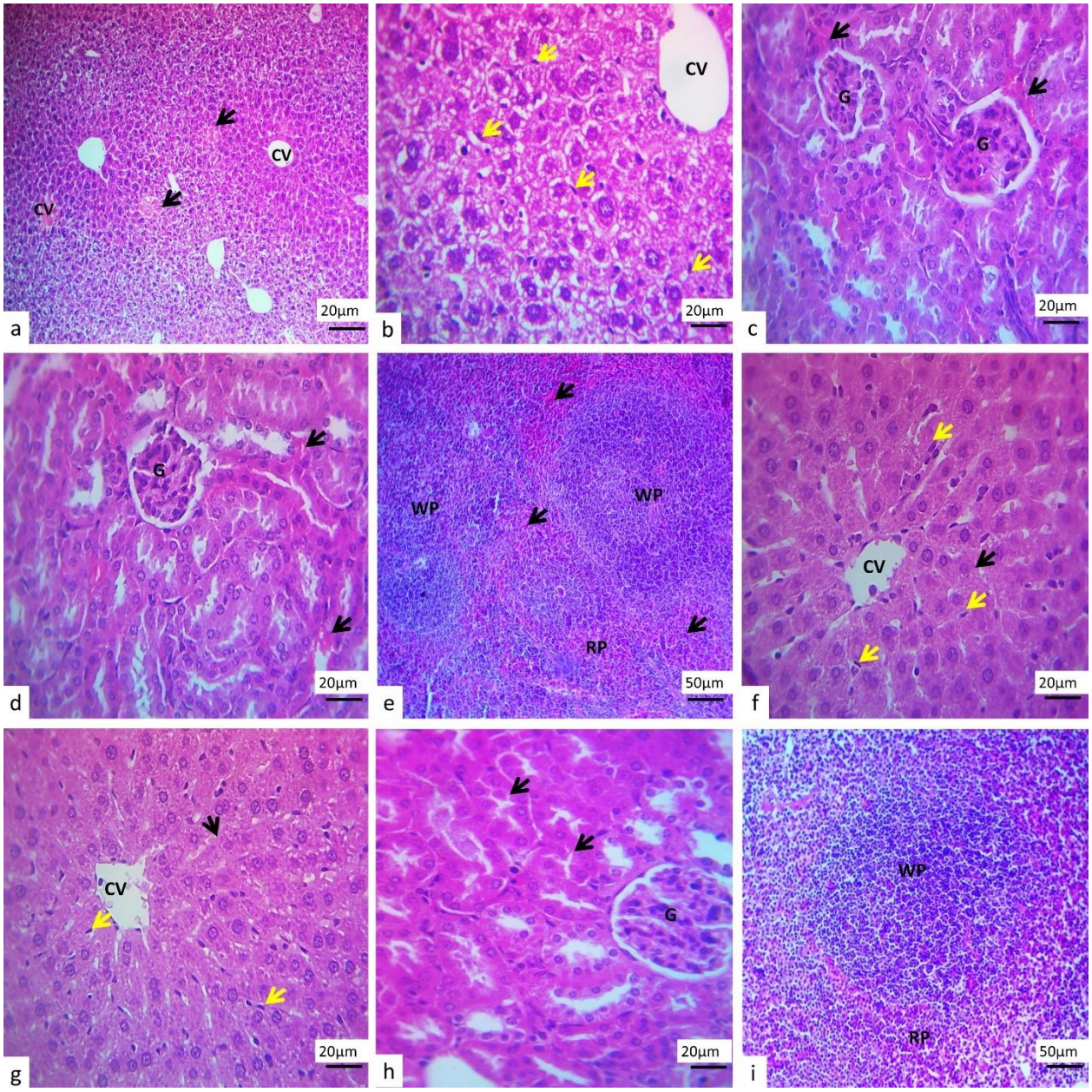

Fig. 4: Light microscopy of histological liver, kidney, and spleen sections of rats in EtOH +treated and control-treated groups showed; a and b: Marked hydropic degeneration of hepatocytes with narrowing of sinusoidal capillary and congestion of central vein (black arrows), the proliferation of Kupffer cells (yellow arrows) in EtOH +Red GSE group, c, and d: Moderate degeneration of collecting tubules with mild interstitial hemorrhage (black arrows) in EtOH +Red GSE group, e: Moderate lymphocytic hyperplasia of white pulp with mild congestion (black arrows), in EtOH +Red GSE group, f and g: Slight hepatocytes swelling (black arrows) with normal organization, Kupffer cells (yellow arrows) in the control-treated group, h: Slight swelling (black arrows) to normal histo-architecture of renal tissue in the control-treated group, i: Normal cellularity and vasculature of splenic parenchyma in the control-treated group, (H&E stain).

cytoplasmic staining (score 9) which was diffusely expressed (Fig. 5f).

Also, in the control positive group, the claudin-1 expression reduced in the kidney parenchyma, and only the cytoplasm of collecting tubules epithelial cells (Fig. 5g) showed diffuse weak staining (score 3) vs. to the claudin-5 that diffusely (score 9) found in the epithelium of the renal tubules by moderate cytoplasmic staining (Fig. 5h). Regarding the E-cadherin expression was decreased and showed weak staining (score 3) but diffusely distributed among the collecting epithelium cytoplasm (Fig. 5i).

The spleen section displayed a range of expressions: in the positive control group, a focal-strong positive reaction (score 5, Fig. 5j) was recorded for claudin-1 vs. claudin-5, which was focally distributed among the parenchyma with moderate intensity (score 3), primarily in white pulp macrophages (Fig. 5k). Conversely, E-cadherin expressed in moderate-strong staining, with the positive cells focally expressed in the white pulp macrophage (score 8) as shown in Fig. 5l.

In comparison to control negative and control positive groups, the Red GSE enhances the expression of the cellular junction's biomarkers mostly in the membranous as a normal pattern; regarding the claudin-1, moderate staining (score 9) diffusely found in the hepatocytes and the renal collecting tubule epithelium, and splenic parenchyma mostly in the venous sinusoid respectively (Fig. 6a-c). While the claudin-5 expression seen in the membrane-cytoplasmic pattern in a moderate- strong intensity staining

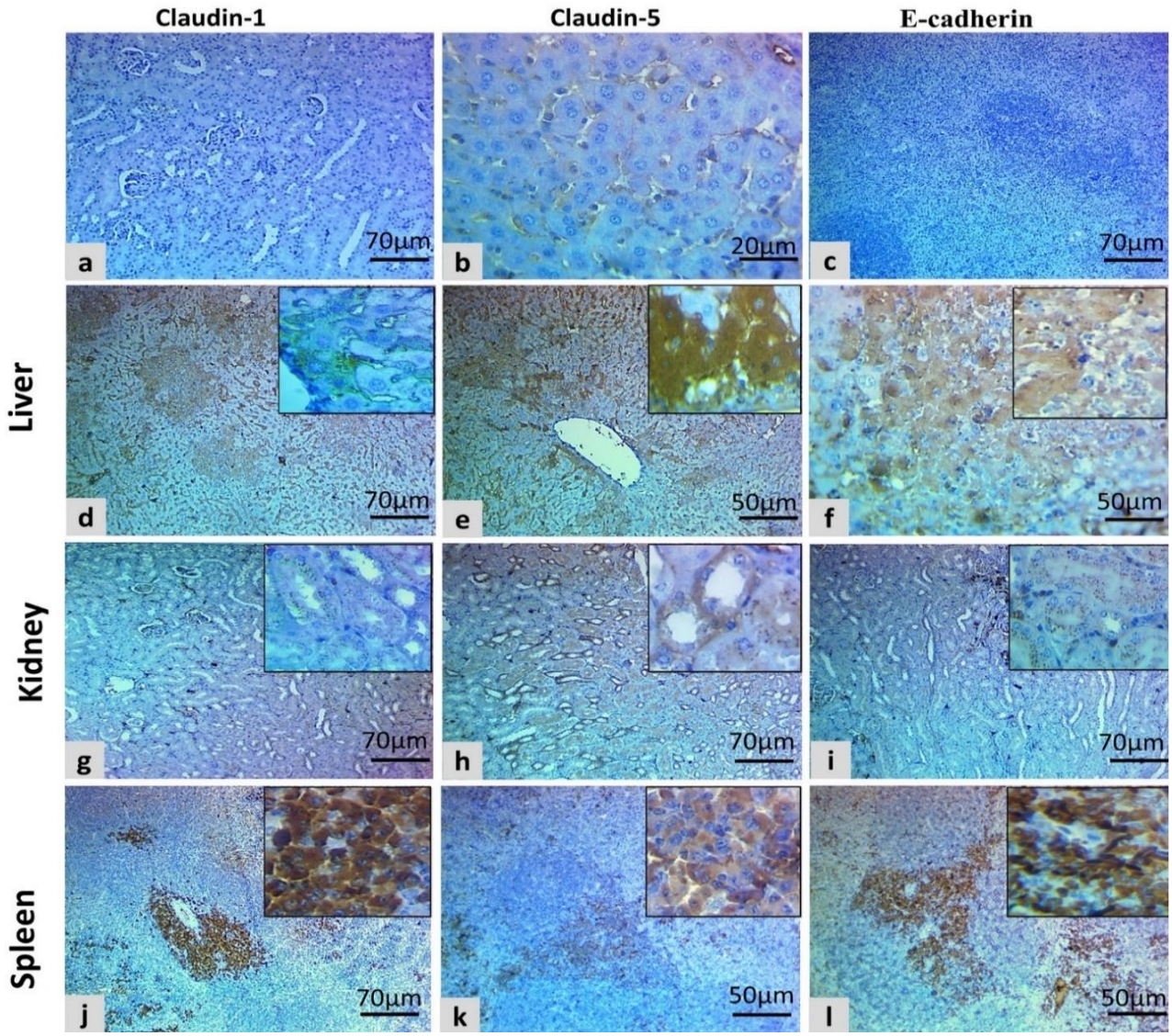

Fig. 5: Immunohistochemical staining of Claudin-1, Claudin-5, and E-cadherin membranous- cytoplasmic immunostaining of a liver, kidney, and spleen tissue sections of the rat. a: Negative staining (score 0) in the control negative group, b: Focal weak membranous endothelial and hepatocyte staining (score 1) in the control negative group, c: Negative staining (score 0) in the control negative group, d: Diffuse weak-moderate staining (score 6) in the control positive group, e, and f: Diffuse moderate staining (score 9) in the control positive group. g: Diffuse weak staining (score 3) in the control positive group, h: Diffuse moderate staining (score 9) in the control positive group. i: Diffuse weak staining (score 3) in the control positive, j: Focal strong staining (score 5) in the control positive. k: Focal moderate staining (score 3) in the control positive. l: Focal moderate-strong staining (score 8) in the control positive.

particularly for the liver section (score12), diffusely expressed also in the kidney and spleen in a weak-moderate pattern (score 6) more specifically in macrophages of the splenic white pulp and the venous endothelium (Fig. 6d-f). Regarding the E-cadherin biomarker in the hepatocyte (Fig. 6g) diffusely expressed in the membrane by moderate staining (score 9) in comparison to the kidney and splenic tissue, which weak-moderate staining diffusely (Fig. 6h & i) expressed in the cytoplasm of the collecting tubules also in macrophages of the splenic white pulp and the venous sinusoid (score 6).

The Red GSE enhanced the tight junction expression in the treatment group; the claudin-1 was diffusely expressed (Fig. 6j & k) by moderate intensity in the liver and kidney (score 9), while it was weakly expressed in the most splenic parenchyma (score 3), (Fig. 6l). Concerning the claudin-5 in the liver section showed moderate staining (Fig. 6m) and diffusely expressed (score 6) vs. to the kidney section which was diffusely expressed in large extent (Fig. 6n) by moderate staining (score 9), while diffusely distributed in the splenic tissue particularly in the white pulp (Fig. 6o) of the spleen by weak staining (score 2). Finally, the E-cadherin in both the liver and kidney diffusely expressed (Fig. 6p & q) in weak-moderate staining (score 6) vs. the splenic section (Fig. 6r) which was moderate staining (score 3) only in the white pulp.

DISCUSSION

An increasing number of studies indicate that consuming too much ethanol might harm the liver, which exacerbates alcohol-related liver disease (ALD) (Younossi *et al.*, 2020). Chronic ethanol consumption has an impact on kidney filtration, yet alcoholism is typically thought of as a hepatic condition. Despite this, the mortality of patients hospitalized with alcoholic hepatitis corresponds with the sudden onset of kidney impairment rather than the underlying hepatitis (Altamirano *et al.*, 2012).

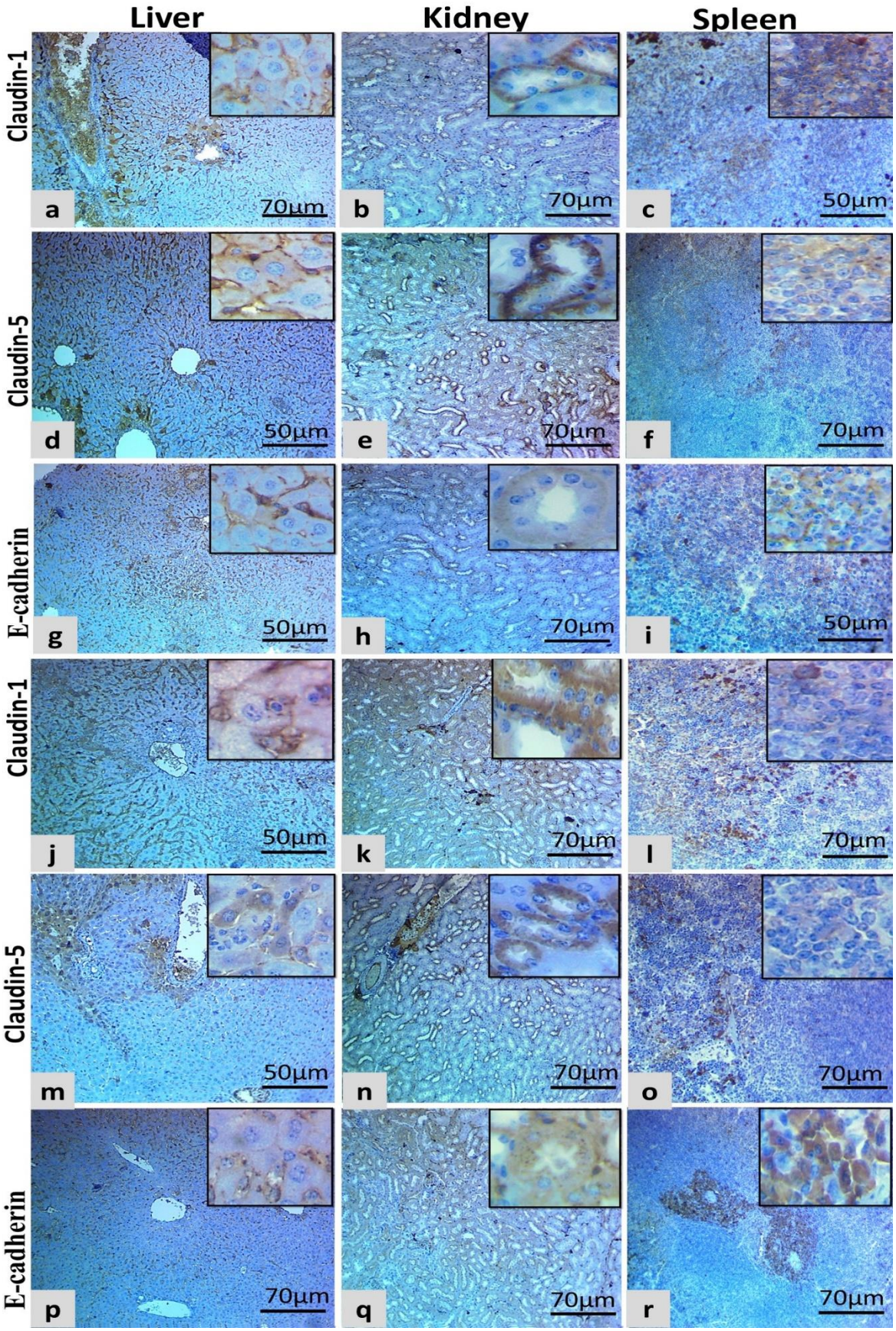

Fig. 6: Immunohistochemical staining of Claudin-1, Claudin-5, and E-cadherin membranous- cytoplasmic immunostaining of a liver, kidney, and spleen tissues of the rat. a-c: Diffuse moderate (score 9) in the control-treated group. d-f: Diffuse moderate-strong (score 12) in the control-treated group. g: Diffuse moderate staining (score 9) in the control-treated group. h and i: Diffuse weak-moderate staining (score 6) in the control-treated group. j and k: Diffuse moderate staining (score 9) in the EtOH+ Red GSE group. l: Diffuse weak staining (score 3) in the EtOH+ Red GSE group. m: Diffuse moderate staining (score 6) in the EtOH+Red GSE group. n: Diffuse moderate staining (score 9) in the EtOH+ Red GSE group o: Diffuse weak staining (score 2) in the EtOH+ Red GSE group. p and q: Diffuse weak-moderate staining (score 6) in the EtOH+ Red GSE group, r: Focal moderate staining (score 3) in the EtOH+ Red GSE group.

According to our research, alcohol-induced chronic hepatitis with significant hepatic necrosis was present in the control-positive group. According to earlier research ethanol causes liver lesions by increasing the cellularity of Kupffer cells (KCs), activated KCs release a lot of ROS and inflammatory mediators, which furthers hepatic damage mediators (Teschke, 2018). Increased lipid peroxidation, the creation of lipid radicals, and a reduction in hepatic antioxidant defense are all factors in ethanol-induced liver injury. The pathophysiology of this process is heavily influenced by oxidative stress (Altamirano *et al.*, 2012). Additionally, an increase in inflammatory infiltration in the livers was a significant side effect of the ethanol administration. In our study, Red GSE administration decreased the harmful effects of ethanol and decreased the severity of score lesions. The explanation for this result is based on a previous study and involves the scavenging of ROS production, which protects the DNA from oxidative damage and attenuation of inflammatory reactions by GSE (Liu *et al.*, 2020). The current investigation aligns with earlier findings that validated the significant beneficial impact of GSE through the Wnt/β-catenin signaling pathway on inflammation and liver cell apoptosis (Sun *et al.*, 2022). The study of Dogan and Celik (2012), proved the positive effect of GSE in attenuating ethanol injury only by biochemical analysis of liver enzyme and antioxidant parameters detection (Dogan and Celik, 2012). Similar to our finding in a model of EtOH-induced liver damage in rats, the previous study revealed that used grape leaf extract inhibits inflammation and produces antioxidant effects, both of which are important in reducing apoptosis and related liver injury (Amen, 2020).

The present data discover a much more serious impact on the kidney, with significant interstitial hemorrhage and obvious interstitial nephritis. Along with it, there was focal glomerular atrophy, which is crucial for the development of acute kidney failure (AKF). In line with earlier findings, proved that leukocyte recruitment and activation were linked to kidney injury induced by ethanol. Both monocytes and neutrophils have the PAF receptor, also the rise in myeloperoxidase mRNA and its enzyme activity is important in a number of kidney disorders (Elgendy *et al.*, 2022). Our results showed that Red GSE reduced the inflammatory reaction and kidney injury. In accordance with our study, only one data documented the effect of GSE in improving kidney function in human patients who suffered from chronic kidney disease (Turki *et al.*, 2016). Also, these findings agree with results that reported that oral administration of grape seed extract ameliorated and enhanced the antioxidant defense against dexamethasone-induced oxidative stress in the kidney and liver (Hasona *et al.*, 2017).

Our findings were corroborated by a study (Aldahmash and El-Nagar, 2013; Lee and Seo, 2021) that provided information on the expansion of the white pulp and increasing splenic diameter. As a result, we looked into the harmful effects of ethanol on the spleen, which lead to splenomegaly and lymphocytic hyperplasia with an increase in immune cells. Disagreement with another study that revealed, in young adult rats, ethanol for 4 weeks increased the plasma pro-inflammatory cytokines, but histologically there were no pathologic signs (Pavón *et al.*, 2016). In the present result, the administration of the Red GSE additionally attenuated the splenomegaly and congestion in the treated group. Our study is the first data proving the attenuation impact of red grape seed extract on the injurious effect of ethanol.

In the present study, the immunohistochemical data showed that ethanol-induced downregulation and translocation of TJ proteins, including Claudin-1, Claudin-5, and E-cadherin compared to the control negative and treatment groups. The Claudin-1 and Claudin-5 in the liver and the kidney sections expressed in a weak-moderate intensity and it was demonstrated that the ethanol-induced decrease in their expression levels was associated with the evoke damage of the tight junction and severity of the lesions, which is consistent with earlier data improved that Claudin-1 and Claudin-5 are essential for the formation and maintenance of a functional barrier. Our results add to the growing body of evidence showing that ethanol-induced loss of TJs integrity causes the noticeable damage and inflammatory response found in the control positive group. This was demonstrated by research in which the elevation of histone acetylation in conjunction with the loss of TJ integrity has been mainly identified as one of the mechanisms behind ethanol-induced barrier failure (Elamin *et al.*, 2012).

According to this data, dysregulation of TJs in kidney sections was primarily found in the proximal and distal tubules rather than in the glomeruli, and the results showed that this increased paracellular transport of solutes and water occurs with increased levels of pro-inflammatory cytokines and elicits a variety of diseases (Krug *et al.*, 2014). The glomerulus did not express claudin; 1, 2, 4, or 5; only the distal and proximal tubules did (Hwang *et al.*, 2014).

These observations are based on the knowledge that damage in ethanol-fed animals correlated with the recruitment and activation of leukocytes (macrophages), which play a crucial role in all phases of the inflammatory responses, even though Claudin-1 and Claudin-5 are strongly expressed in the macrophage of the splenic parenchyma (Matin *et al.*, 2022). Our data are the first study to focus on the effect of ethanol-induced modulation of the E-cadherin expression in the liver, kidney, and spleen and play a critical role in accelerating the severity of the cellular injury and inflammation; interestingly, the immunohistochemical data of E-cadherin also had the same pattern in expression as Claudin-1 and Claudin-5 in the liver and kidney expressed weak-moderate while in the spleen moderately stained, similar to the study that documented E-cadherin has been recognized as one of the key factors to maintaining the morphological structure and functional integrity of epithelial cells (Chen *et al.*, 2019). In the present study, the E-cadherin expression was strongly higher in the macrophages of the splenic white pulp therefore the severity of the inflammation was higher, the other hypothesis is M1 macrophage infiltration is thought to be the primary cause of the secondary injury cascade due to releasing iNOS and TNF (Klingener *et al.*, 2014).

Our ongoing research aims to determine whether Red GSE can reduce the damaging effects of ethanol on the liver, kidney, and spleen. In the group that was only treated with 6 Red GSE and the EtOH+ Red GSE group, the markers were highly expressed in a normal pattern. They

were primarily membranous, in contrast to the control positive group, whose TJ biomarkers and an adherent junction protein (E-cadherin), while claudin-5 expression is detected in the kidney and spleen in a weak-moderate pattern in macrophages and the splenic white pulp as well as in the venous endothelium, it is also seen in the hepatocytes where it is stained with a moderate-strong intensity. Our study is the first attempt to use Red GSE on the TJ in the liver, kidney, and spleen, our findings regarding the E-cadherin biomarker in the hepatocytes, which showed moderate staining compared to weak to moderate staining in the kidney and splenic tissue, is the first data that has proven till now, and there is no study related to the intercellular junction and GSE.

Conclusions: This study provides evidence that Red GSE, a naturally occurring chemical, can strengthen TJs and modulate the expression of intercellular junction proteins. This greatly advances our understanding of Red GSE's role in correcting detrimental agents on the intercellular junction that are caused by a range of causes including the radiation, stress, and microbiological agents that induce the disease and progress to cancer.

Acknowledgments: This work was reinforced by the College of Veterinary Medicine, University of Sulaimani, Sulaymaniyah, Iraq. This project was not supported by any agency or organization.

REFERENCES

Aldahmash BA and El-Nagar DM, 2013. Histological study on the hazardous effects of ethanol on liver and spleen in Swiss albino mice. J Soci Deve New Net Environ in B & H (7):2445-2452.

Altamirano J, Fagundes C, Dominguez M, et al., Acute kidney injury is an early predictor of mortality for patients with alcoholic hepatitis. 2012. Clin Gastroenterol Hepatol 10:65-71. e63.

Amen YS, 2020. Grape-leaf extract attenuates alcohol-induced liver injury via interference with the NF-κB signaling pathway. Biomolecules 10: 550-558.

Benmeziane F, Djamai R, Cadot Y, et al., 2014. Optimization of extraction parameters of phenolic compounds from Algerian fresh table grapes, (Vitis vinifera). Intern Food Res J 1:14-21.

Chen D, Hu S, Liu J, et al., 2019. E-cadherin regulates the biological behaviors of neural stem cells and promotes motor function recovery following spinal cord injury. Exp Ther Med 17:2061-2070.

Chiasson-MacKenzie C and McClatchey AI, 2018. Cell-cell contact and receptor tyrosine kinase signaling. Cold Spring Harb Perspect Biol 10:a029215.

Dogan A and Celik I, 2012. Hepatoprotective and antioxidant activities of grape seeds against ethanol-induced oxidative stress in rats. Br J Nutr 107: 45-51.

Elamin E, Jonkers D, Juuti-Uusitalo K, et al., 2012. Effects of ethanol and acetaldehyde on tight junction integrity: in vitro study in a three-dimensional intestinal epithelial cell culture model. PloS One 7: e35008.

Elgendy SA, Baloza SH, Mohammed LA, et al., 2022. Ameliorative impacts of wheat germ oil against ethanol-induced hepatic and renal dysfunction in rats: involvement of anti-inflammatory, antiapoptotic, and antioxidant signaling pathways. Life 12:1668-1671.

Hasona NA, Alrashidi AA, Aldugieman TZ, et al. 2017. Vitis vinifera extract ameliorates hepatic and renal dysfunction induced by dexamethasone in albino rats. Toxics 5:1-11.

Hassan S, Hassan SN and Maarof NN, 2021. Clinical and Histopatho-logical study of black and Red Grape Seed extracts (Vitis Vinifera) effects on the Albino Mice. India J Forensic Med Toxicol 15.

Hassan SM, Saeed AK and Hussein AJ, 2015. Ethanol-induced hepatic and renal histopathological changes in BALB/c mice. J Nat Sci Res 2015;5:2224-3186.

Hassan SMA, Saeed AK, Rahim OO, et al., 2022. Alleviation of cisplatin-induced hepatotoxicity and nephrotoxicity by L-carnitine. Iran J Basic Med Sci 25:897.

Hintermann E and Christen U, 2019. The many roles of cell adhesion molecules in hepatic fibrosis. Cells 8:1503.

Hwang I, Yang H, Kang HS, et al., 2014. Spatial expression of claudin family members in various organs of mice. Mol Med Rep 9:1806-1812.

Klingener M, Chavali M, Singh J, et al., 2014. N-cadherin promotes the recruitment and migration of neural progenitor cells from the SVZ neural stem cell niche into demyelinated lesions. J Neurosci 34:9590-9606.

Koda R, Zhao L, Yaoita E, et al., 2011. Novel expression of claudin-5 in glomerular podocytes. Cell Tissue Res 343:637-648.

Krug SM, Schulzke JD and Fromm M, 2014. Tight junction, selective permeability, and related diseases. Semin Cell Dev Biol 4: 166-176.

Lee JH and Seo B-I, 2021. Effects of Akebia quinata extract on alcohol-induced damage of liver, spleen, and thymus in rats. Korea J Herbol 36:11-17.

Liu M, Yun P, Hu Y, et al., 2020. Effects of grape seed proanthocyanidin extract on obesity. Obes Facts 13:279-291.

Li Y, Zhu B, Song, N, Shi, et al., 2022. Alcohol consumption and its association with chronic kidney disease: Evidence from a 12-year China Health and Nutrition Survey. Nutr Metab Cardiovasc Dis 32: 1392-1401.

Matin MA, Hossen MJ, Ahmed MS, et al., 2022. The role of macrophages in inflammation. In: Recent Advance in Micro Diversity. 1st Ed, Elsevier, USA, pp:53-71.

Menezes L, Fioravanti M, Oliveira F, et al., 2017. Histological evaluation and E-cadherin and β-catenin expression in the kidney of dogs submitted to renal ischemia and reperfusion after chlorpromazine administration. Arq Bras de Med Vet e Zoo 69:1206-1214.

Müller L, Hatzfeld M, Keil R, et al., 2021. Desmosomes as signaling hubs in the regulation of cell behavior. Front Cell Dev Biol 9: 1-22.

Mukherji A, Bailey SM, Staels B, et al., 2019. The circadian clock and liver function in health and disease. J Hepatol 71:200-211.

Mustafa HH, Hassan S, Mohammed SA, et al., 2022. The Effect of Egg Yolk Oil in Repairing Tight Junction Claudin-1 in Periodontitis in a Wistar Rat. P V J 42:467-474.

Nagy LE, Ding WX, Cresci G, et al., 2016. Linking pathogenic mechanisms of alcoholic liver disease with clinical phenotypes. Gastroenterol 150:1756-1768.

Pavón FJ, Marco EM, Vázquez M, et al., 2016. Effects of adolescent intermittent alcohol exposure on the expression of endocannabinoid signaling-related proteins in the spleen of young adult rats. PloS one 11:e0163752

Pradhan ST, Zhou L, Vats R, et al., 2018. Dual catenin loss in the murine liver causes tight junctional deregulation and progressive intrahepatic cholestasis. Hepatol 67:2320-2337.

Ramkissoon R and Shah VH, 2022. Alcohol use disorder and alcohol-associated liver disease. Alcohol Res: Curr Rev 42:1-9.

Shim Y-R and Jeong W-I, 2020. Recent advances of sterile inflammation and inter-organ cross-talk in alcoholic liver disease. Exp Mole Med 52: 772-780.

Singh AB, Uppada SB, and Dhawan P, 2017. Claudin proteins, outside-in signaling, and carcinogenesis. Pflügers Arch-Eur J Physiol 469:69-75.

Sun HY, Gu AX, Huang BY, et al., 2022. Dietary grape seed proanthocyanidin alleviates the liver injury induced by long-term high-fat diets in Sprague Dawley rats. Front Vet Sci 9:959999-959906.

Surai P, 2014. Polyphenol compounds in the chicken/animal diet: from the past to the future. J Anim Physiol Anim Nutr 98:19-31.

Tamargo C, Hanouneh M, Cervantes CE, et al., 2024. Treatment of Acute Kidney Injury: A Review of Current Approaches and Emerging Innovations. J Clin Med13: 2449-2455.

Teschke R, 2018. Alcoholic liver disease: alcohol metabolism, cascade of molecular mechanisms, cellular targets, and clinical aspects. Biomed 6:100-106.

Turki K, Charradi K, Boukhalfa H, et al., 2016. Grape seed powder improves renal failure in chronic kidney disease patients. EXCLI J 15:420-424.

Younossi ZM, Stepanova M, Younossi Y, et al., 2020. Epidemiology of chronic liver diseases in the USA in the past three decades. Gut 69:564-568.

Zeisel MB, Dhawan P, and Baumert TF, 2019. Tight junction proteins in gastrointestinal and liver disease. Gut 68:547-561.

Zhang Y-J, Gan R-Y, Li S, et al., Antioxidant phytochemicals for the prevention and treatment of chronic diseases. Mol 2015;20:21138-21156.